

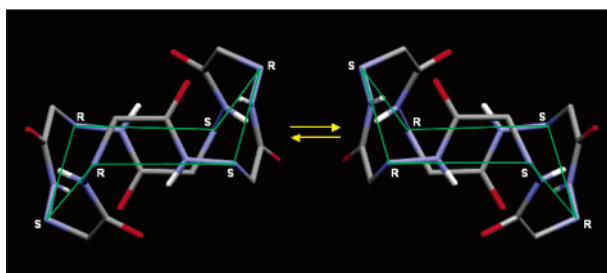
## Aza- $\beta^3$ -Cyclohexapeptides: Pseudopeptidic Macrocycles with Interesting Conformational and Configurational Properties Slow Pyramidal Nitrogen Inversion in 24-Membered Rings!

Philippe Le Grel,<sup>\*,†</sup> Arnaud Salaün,<sup>†</sup> Michel Potel,<sup>‡</sup> Barbara Le Grel,<sup>†</sup> and Frédéric Lassagne<sup>†</sup>

ICMV, UMR CNRS 6226, Université de Rennes I, 263 avenue du Général Leclerc 35042 Rennes Cedex, France, and CSM, UMR CNRS 6226, Université de Rennes I, 263 avenue du Général Leclerc 35042 Rennes Cedex, France

philippe.legrel@univ-rennes1.fr

Received April 22, 2006



Among pseudopeptidic foldamers, aza- $\beta^3$ -peptides have the unique property to possess nitrogen stereocenters instead of carbon stereocenters. As the result of pyramidal inversion at  $N^\alpha$ -atoms along the backbone, they behave as a set of  $C_8$ -based secondary structures in equilibrium. This structural modulation is exploited here to prepare 24-membered macrocycles with great efficiency. Both crystal structures and spectroscopic data establish that aza- $\beta^3$ -cyclohexapeptides adopt a highly organized conformation where the relative configuration of chiral nitrogen atoms is alternated. This makes them an interesting scaffold as the stereocontrol occurs spontaneously through the cyclization. These compounds reveal an unprecedented slow pyramidal nitrogen inversion in macrocycles. Pyramidal ground state stabilization, hindered rotation, steric crowding, and H-bond cooperativity are proposed to participate in this striking phenomenon. The equilibrium between invertomers of aza- $\beta^3$ -cyclohexapeptides is reminiscent of the interchange between the two chair forms of cyclohexane.

### Introduction

The replacement of an  $\alpha$ -amino acid by an  $\alpha$ -hydrazino acid (Figure 1) is one of the oldest modifications to have been introduced into a peptidic sequence.<sup>1</sup> In contrast, true hydrazinopeptides, namely, oligomers of  $\alpha$ -hydrazino acids, have been described only within the past few years.<sup>2</sup> Currently, despite several improvements,<sup>3</sup> high-scale synthesis of optically pure  $\alpha$ -hydrazino acids and the subsequent coupling steps remain laborious.

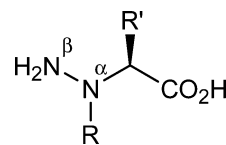


FIGURE 1.  $\alpha$ -Hydrazino acid.

The revival of hydrazinopeptides is related to the current interest in biomimetic oligomers. In particular, Günther and Hofmann recently showed their potential in the extension of the  $\beta$ -peptide concept by describing the variety of secondary structures they could adopt<sup>4</sup> and calculating the relative energies associated with them.

In 2003, Seebach and Lelais hardly succeeded in preparing a series of optically pure hydrazinopeptides ( $R' \neq H$ ,  $R = H$ ;

<sup>†</sup> ICMV.

<sup>‡</sup> CSM.

(1) (a) Niedrich, H. *Chem. Ber.* **1967**, *100*, 3273. (b) Niedrich, H. *Chem. Ber.* **1969**, *102*, 1557.

(2) (a) Cheguillaume, A.; Salaün, A.; Sinbandhit, S.; Potel, M.; Gall, P.; Baudy-Floc'h, M.; Le Grel, P. *J. Org. Chem.* **2001**, *66*, 4923. (b) Lelais, G.; Seebach, D. *Helv. Chim. Acta* **2003**, *86*, 4152.

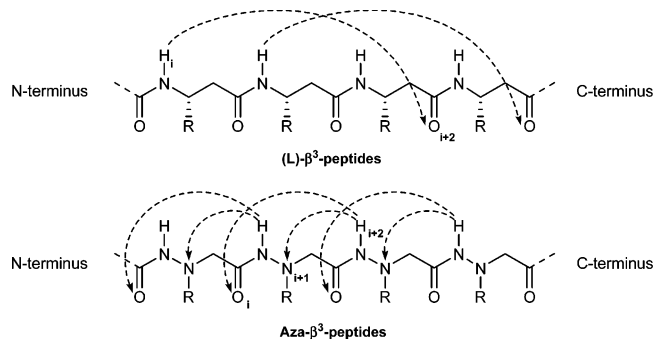


**FIGURE 2.** Comparison between hydrogen-bond network of  $\beta^3$ -peptides and that of aza- $\beta^3$ -peptides.

3-aza- $\beta^2$ -peptides) ranging from the dimer to the hexamer. Circular dichroism curves are compatible with folding, but these compounds proved to be resistant to classical NMR conformational analysis, and the secondary structure remain undetermined.<sup>2b</sup>

We are engaged in the synthesis and structural study of aza- $\beta^3$ -peptides,<sup>2a</sup> which are special hydrazinopeptides with the side chains located on the pyramidal  $N^\alpha$  nitrogen atoms. Because the difficulties associated with the handling of chiral  $\alpha$ -hydrazino acid building blocks are avoided, aza- $\beta^3$ -peptides can be prepared on large scale using classical coupling procedures (EDCI/HOBT) from the readily accessible  $N^\alpha$ -substituted hydrazinoacetic acid derivatives ( $R' = H$ ,  $R \neq H$ ).<sup>5</sup>

Aza- $\beta^3$ -peptides are sterically comparable with the corresponding  $\beta^3$ -peptides (Figure 2), which undergo spontaneous contraction as a result of H-bond contacts between  $H_i$  and  $O_{i+2}$ . The resulting network of 14-membered hydrogen-bonded pseudocycles ( $C_{14}$ ) stabilizes the well-known  $3_{14}$ -helix.<sup>6</sup> In contrast, the replacement of the  $\beta$ -carbons by nitrogen atoms induces a full reorganization of the H-bond network, on the basis of repeated  $C_8$  pseudocycles.<sup>2a</sup> Actually, in this position, the lone pair of the nitrogen atoms ( $N_{i+1}$ ) readily forms a H-bond with the neighboring hydrazidic  $NH_{i+2}$ , which favors further H-bonding between the hydrazidic  $NH_{i+2}$  and the oxygen of  $CO_i$ . Consequently, the  $C_8$  pseudocycles involved in the secondary structure of aza- $\beta^3$ -peptides are a bifidic hydrogen-bonded system, called hydrazinoturns, where the hydrazidic  $NH_{i+2}$  equilibrates between the two H-bond acceptors (Figure

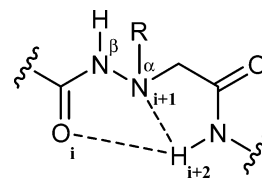


**FIGURE 3.** Hydrazinoturn, a bifidic hydrogen-bonded  $C_8$  pseudocycle.

3).<sup>7</sup> A similar  $C_8$ -based organization<sup>8</sup> has also been postulated for the structurally related oxa-peptides.<sup>9</sup> It should be noted that  $C_8$ -based secondary structures have also been demonstrated for  $\beta^{2,2}$ -peptides<sup>10</sup> of 1-(aminomethyl)cyclopropane carboxylic acid and for (2*R*,3*S*)- $\beta^{2,3}$ -peptides<sup>11</sup> bearing a hydroxyl group on carbon atoms in position 2. In these two cases, additional interactions also stabilize the  $C_8$  pseudocycles.

From the crystal structures of several aza- $\beta^3$ -peptides,<sup>12</sup> illustrated here in the case of an hexamer (Figure 4a), we could extract the average values of torsional angles  $\omega$ ,  $\phi$ ,  $\theta$ , and  $\psi$  that characterized a hydrazinoturn (Figure 4b and Table 1). In a hydrazinoturn, the absolute configuration of the  $N^\alpha$  atom is either *R* (*R*-hydrazinoturn) or *S* (*S*-hydrazinoturn). The interchange between the two forms requires not only pyramidal inversion of the  $N^\alpha$  atom but also  $\pi$  rotation around the  $N^\beta$ - $N^\alpha$  and  $N^\alpha$ - $C_\alpha$  bonds.

The hydrazidic linkage is forced in the *Z* geometry ( $\omega \approx 180^\circ$ ) by the NH to CO H-bond. The value of  $\phi$  is governed by the minimization of lone pair electron repulsion between the two adjacent nitrogen atoms (Figure 5a), while those of  $\theta$  correspond to a (+)-synclinal or (-)-synclinal conformation, which places the R substituent on the  $N^\alpha$  atom in a favorable free zone of space (Figure 5b). The low value of  $\psi$  results from the H-bond between  $NH_{i+2}$  and  $N^\alpha_{i+1}$  (Figure 5c).

The combination of the trans geometry of the hydrazidic linkage ( $\omega \approx 180^\circ$ ) with the low value of  $\psi$  induces a near perfect planarity of the molecular segments between two successive stereocenters (Figure 6). As a result, aza- $\beta^3$ -peptides can be depicted as a succession of planes, joined together by the chiral nitrogen atoms. From this point of view, aza- $\beta^3$ -peptides resemble  $\alpha$ -peptides, in which the planar peptidic bonds are connected by the  $\alpha$ -carbons. However, they differ from peptides in that the relative orientation of two successive planes is further limited by the H-bond between  $NH_{i+2}$  and the oxygen of  $CO_i$ .

Among foldamers, aza- $\beta^3$ -peptides are unique in possessing nitrogen stereocenters instead of carbon stereocenters. Although the framework of hydrazinoturns clearly folds the backbone, it does not sustain a single secondary structure in solution because

(3) (a) Pollak, G.; Yellin, H.; Carmi, A. *J. Med. Chem.* **1964**, *7*, 220. (b) Klosterman, H. J.; Lamoureux, G. L.; Parsons, J. L. *Biochemistry* **1967**, *6*, 170. (c) Lijinsky, W.; Keefer, L.; Loo, J. *Tetrahedron* **1970**, *26*, 5137. (d) Achiwa, K.; Yamada, S. *Tetrahedron Lett.* **1975**, *16*, 2701. (e) Gennari, C.; Colombo, L.; Bertolini, G. *J. Am. Chem. Soc.* **1986**, *108*, 6394. (f) Evans, D. A.; Britton, T. C.; Dorow, R. L.; Delaria, J. F. *J. Am. Chem. Soc.* **1986**, *108*, 6395. (g) Trimble, L. A.; Vederas, J. C. *J. Am. Chem. Soc.* **1986**, *108*, 6397. (h) Viret, J.; Gabard, J.; Collet, A. *Tetrahedron* **1987**, *43*, 891. (i) Vidal, J.; Guy, L.; Stérin, S.; Collet, A. *J. Org. Chem.* **1993**, *58*, 4791. (j) Niederer, D. A.; Kapron, J. T.; Vederas, J. C. *Tetrahedron Lett.* **1993**, *34*, 6859. (k) Vidal, J.; Damestoy, S.; Guy, L.; Hannachi, J. C.; Aubry, A.; Collet, A. *Chem.-Eur. J.* **1997**, *3*, 1691. (l) Killian, J. A.; Van Cleve, M. D.; Shayo, Y. S.; Hecht, S. M. *J. Am. Chem. Soc.* **1998**, *120*, 3032. (m) Brosse, N.; Pinto, M. F.; Bodiguel, J.; Jamart-Grégoire, B. *J. Org. Chem.* **2001**, *66*, 2869.

(4) Günther, R.; Hofmann, H.-J. *J. Am. Chem. Soc.* **2001**, *123*, 247. (5) Cheguillaume, A.; Doublil-Bounoua, I.; Baudy-Floc'h, M.; Le Grel, P. *Synlett* **2000**, *3*, 331.

(6) (a) Seebach, D.; Overhand, M.; Kühnle, F. N. M.; Martinoni, B.; Oberer, L.; Hommel, U.; Widmer, H. *Helv. Chim. Acta* **1996**, *79*, 913. (b) Seebach, D.; Ciceri, P. E.; Overhand, M.; Jaun, B.; Rigo, D.; Oberer, L.; Hommel, U.; Amstutz, R.; Widmer, H. *Helv. Chim. Acta* **1996**, *79*, 2043. (c) Seebach, D.; Abele, S.; Gademann, K.; Guichard, G.; Hintermann, T.; Jaun, B.; Matthews, J. L.; Schreiber, J. V.; Oberer, L.; Hommel, U.; Widmer, H. *Helv. Chim. Acta* **1998**, *81*, 932.

(7) Salaün, A.; Favre, A.; Le Grel, B.; Potel, M.; Le Grel, P. *J. Org. Chem.* **2006**, *71*, 150.

(8) Thevenet, L.; Vanderesse, R.; Marraud, M.; Didierjean, C.; Aubry, A. *Tetrahedron Lett.* **2000**, *41*, 2361.

(9) (a) Yang, D.; Ng, F.-F.; Li, Z.-J.; Wu, Y.-D.; Chan, K. W. K.; Wang, D.-P. *J. Am. Chem. Soc.* **1996**, *118*, 9794. (b) Yang, D.; Qu, J.; Li, B.; Ng, F.-F.; Wang, X.-C.; Cheung, K.-K.; Wang, D.-P.; Wu, Y.-D. *J. Am. Chem. Soc.* **1999**, *121*, 589. (c) Wu, Y.-D.; Wang, D.-P.; Chan, K. W. K.; Yang, D. *J. Am. Chem. Soc.* **1999**, *121*, 11189. (d) Yang, D.; Li, B.; Ng, F.-F.; Yan, Y.-L.; Qu, J.; Wu, Y.-D. *J. Org. Chem.* **2001**, *66*, 7303. (e) Yang, D.; Qu, J.; Li, W.; Wang, D.-P.; Ren, Y.; Wu, Y.-D. *J. Am. Chem. Soc.* **2003**, *125*, 14452.

(10) Abele, S.; Seiler, P.; Seebach, D. *Helv. Chim. Acta* **1999**, *82*, 1559.

(11) Gademann, K.; Häne, A.; Rueping, M.; Jaun, B.; Seebach, D. *Angew. Chem., Int. Ed.* **2003**, *42*, 1534.

(12) Salaün, A.; Potel, M.; Roisnel, T.; Gall, P.; Le Grel, P. *J. Org. Chem.* **2005**, *70*, 6499.

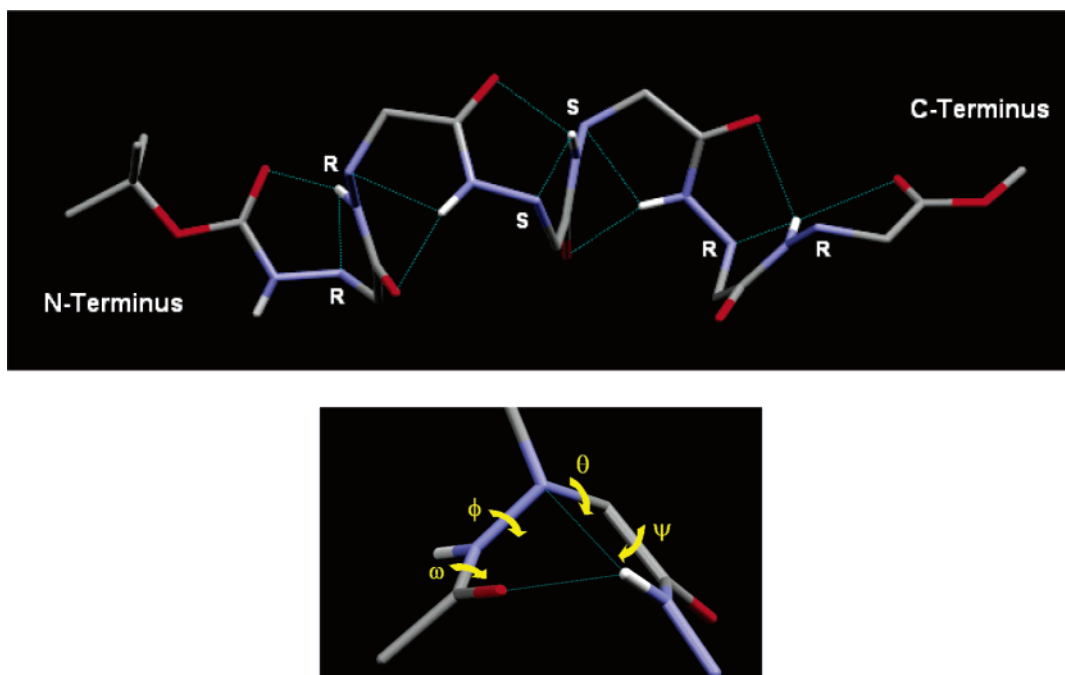


**FIGURE 4.** (Top) Solid state organization of an aza- $\beta^3$ -hexapeptide. The secondary structure is maintained by a framework of hydrazinoturns. Crystallization has selected the *RRSSRR/SSRRSS* chiral sequences. Side chains are omitted for clarity. (Bottom) Torsional angles defining a hydrazinoturn.

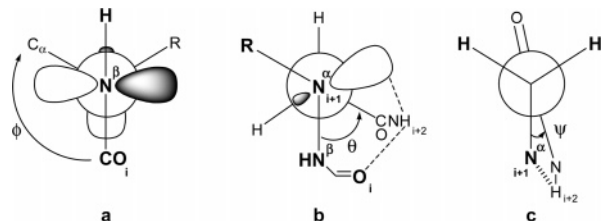


**FIGURE 5.** Schematic Newman projections showing the structural features of a *R*-hydrazinoturn in relation to the angles (a)  $\phi$ , (b)  $\theta$ , and (c)  $\psi$ .

**TABLE 1.** Average Torsional Angles (deg) of an *R*- and an *S*-Hydrazinoturn in Aza- $\beta^3$ -Peptides

torsional angles	$\omega$	$\phi$	$\theta$	$\psi$
<i>R</i> -hydrazinoturn	180	+120	-75	-15
<i>S</i> -hydrazinoturn	180	-120	+75	+15

of the pyramidal inversion of the  $N^\alpha$  nitrogen. Aza- $\beta^3$ -peptides actually behave as a set of secondary structures in equilibrium. Combined with the geometrical constraints of the hydrazinoturn, the chiral sequence of the  $N^\alpha$  nitrogen atoms gives each diastereoisomer a specific shape. A homochiral sequence (all *S* or all *R*) confers to the backbone an elongated conformation, namely, a  $H_8$  helix as described by Günther and Hofmann. Heterochiral sequences further contract the oligomer. In the case of *RSRSRS* (or *SRSRSR*) chiral sequence, the set of dihedral angles associated with the hydrazinoturns defines a conformation which moves closer together the N-terminus and C-terminus. In taking advantage of this principle, the synthesis of  $\alpha$ -peptides with alternating chiral sequence has proven to be successful to favor peptidic macrocyclization.<sup>13</sup> It follows that the conformational specificity of aza- $\beta^3$ -hexapeptides should naturally promote efficient synthesis of the corresponding macrocycles. This work is aimed at checking this prediction. Concomitantly, interesting questions emerge about the relative stereochemistry

that could adopt the  $N^\alpha$  nitrogen atoms into such cyclic compounds.

## Results and Discussion

Macrocycles **1**, **2**, and **3** (Figure 7a) were obtained very cleanly from the deprotected precursors by treatment with an excess of EDCI/HOBT in DCM at 1 mM. They were isolated in very high purity in over 70% yields. These excellent yields can be compared with the synthesis of the comparable oxapeptidic macrocycle (35%) by Yang and Coll (Figure 7b), even though they started from an optically pure  $D,L$ -oxa-hexapeptide.<sup>14</sup> This is especially surprising because the conformation of both aza- $\beta^3$ -peptides and oxa-peptides is believed to rely on similar  $C_8$  pseudocycles. It seems, then, that the specific conformational flexibility of aza- $\beta^3$ -peptides confers a greater efficiency to the macrocyclization.

Compounds **1**, **2**, and **3** were crystallized from acetonitrile, toluene/2-propanol, and 2-propanol, respectively. Despite the diversity of the solvents, X-ray analyses revealed a common organization of the backbone. As in linear precursors, it is structured by a framework of hydrazinoturns, which is here uninterrupted because of the cyclic nature of the compounds. The relative configuration of the  $N^\alpha$  nitrogen atoms is alternated, as they are postulated to be during the cyclization. The side

(13) (a) De Santis, P.; Morosetti, S.; Rizzo, R. *Macromolecules* **1974**, *7*, 52. (b) Khazanovich, N.; Granja, J. R.; McRee, D. E.; Milligan, R. A.; Ghadiri, M. R. *J. Am. Chem. Soc.* **1994**, *116*, 6011. (c) Hartgerink, J. N.; Granja, J. R.; Milligan, R. A.; Ghadiri, M. R. *J. Am. Chem. Soc.* **1996**, *118*, 43. (d) Clark, T. D.; Buehler, L. K.; Ghadiri, M. R. *J. Am. Chem. Soc.* **1998**, *120*, 651. (e) Clark, T. D.; Buriak, J. M.; Kobayashi, K.; Isler, M. P.; McRee, D. E.; Ghadiri, M. R. *J. Am. Chem. Soc.* **1998**, *120*, 8949. (f) Bong, D. T.; Ghadiri, M. R. *Angew. Chem., Int. Ed.* **2001**, *40*, 2163. (g) Rosenthal-Aizman, K.; Svensson, G.; Undén, A. *J. Am. Chem. Soc.* **2004**, *126*, 3372. (h) Ashkenasy, N.; Horne, W. S.; Ghadiri, M. R. *Small* **2006**, *1*, 99.

(14) Yang, D.; Qu, J.; Li, W.; Zhang, Y.-H.; Ren, Y.; Wang, D.-P.; Wu, Y.-D. *J. Am. Chem. Soc.* **2002**, *124*, 12410.

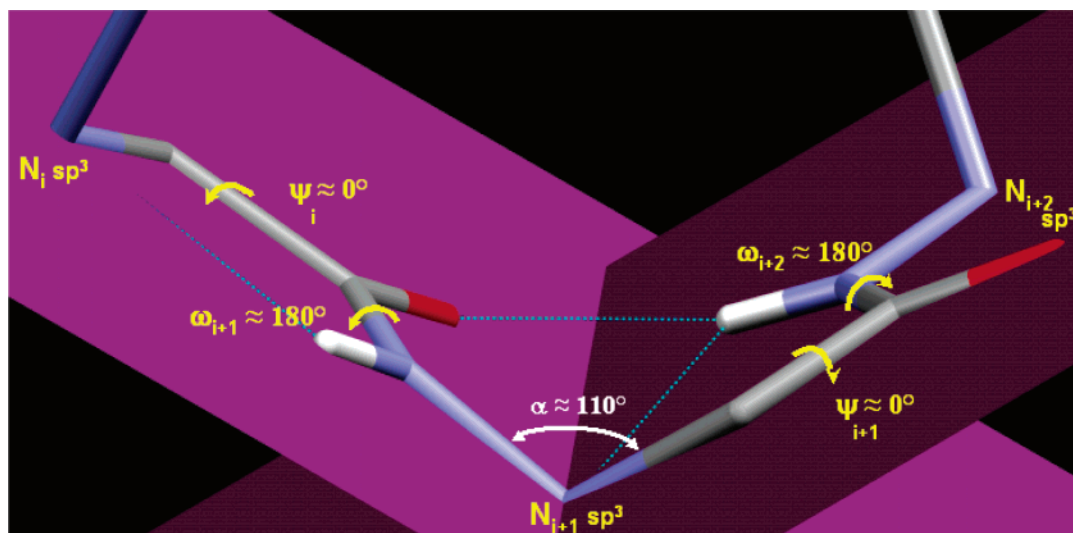


FIGURE 6. Planes defined by the combination of the  $\psi$  and  $\omega$  values.

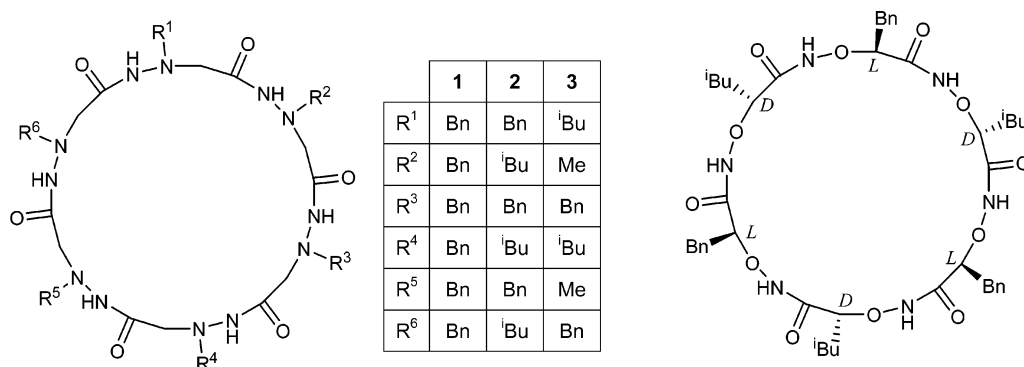


FIGURE 7. (a) 24-membered aza- $\beta^3$ -cyclohexapeptides. (b) 24-membered oxa-cyclohexapeptide.

view in Figure 8a shows that the persistence of the six hydrazinoturns in the cyclic compounds forces the covalent backbone to adopt a wavy structure, with a thickness of around 4.5 Å. The backbone is also characterized by a secant plane which includes the six  $N^{\beta}H$ . Side chains occupy equatorial positions and tend to point alternately toward the top side and the bottom side of the macrocycle. All the *Z* hydrazidic linkages are successively oriented in opposite direction. The top view (Figure 8b) shows that the macrocycle appears in the shape of a nearly perfect hexagonal bracelet. A very similar structure was calculated by Wu and Yang to be the global minimum for their cyclic oxa-hexapeptide.<sup>14</sup> The secondary structure maintained by the H-bond network associated with the set of hydrazinoturns induces a very tight conformation, which reduces the diameter of the internal cavity to around 2.5 Å as illustrated by the van der Waals representation (Figure 8c). For comparison, the diameter of 24-membered cyclic octapeptides is around 6–7 Å.<sup>13c</sup>

The average values of torsional angles  $\omega$ ,  $\phi$ ,  $\theta$ , and  $\psi$ , measured for the macrocycles, are listed in Table 2. The comparison with Table 1 shows that the macrocycles impose only slight angular modulation to the average canonical values observed in the starting aza- $\beta^3$ -peptides. It follows that hydrazinoturns are fully compatible with the cyclic structure.

Table 3 shows the average distances and angles associated with the bifidic H-bond interactions in aza- $\beta^3$ -cyclohexapeptides and the corresponding values observed in aza- $\beta^3$ -peptides. For the cyclic compounds, the characteristics of the  $CO \cdots HN$  bond

are closer to the optimum H-bond distance obtained by statistical surveys of crystallographic data<sup>15</sup> (1.90 Å) and to the ab initio calculated optimum angles for amide–amide hydrogen bonding (160°).<sup>16,17</sup> At the same time, the geometry of the  $N \cdots HN$  bond is almost unaffected.

**Analysis of the Conformation of Aza- $\beta^3$ -Cyclohexamers in  $CDCl_3$ .** Before examining the spectral characteristics of aza- $\beta^3$ -cyclohexapeptides, we focused on *N,N*-dibenzylacetyldrazide<sup>18</sup> **4** (Figure 9) as a model compound, from which we gained useful spectroscopic references. The <sup>1</sup>H NMR spectrum (10 mM,  $CDCl_3$ ) of **4** shows two sets of signals in a 3:1 ratio, which reflect the *E/Z* isomerism of the hydrazidic bond.<sup>19</sup> It has been postulated that the equilibrium is shifted toward the *Z* isomer in polar solvents.<sup>20</sup> In  $DMSO-d_6$ , in fact, the percentage of the minor isomer increases up to 43%. We confirmed its postulated *Z* geometries using NOE measurements. It follows that the chemical shift of the *Z* isomer at 10 mM in  $CDCl_3$  is 6.50 ppm, whereas the corresponding  $\delta NH_E$  is 6.05 ppm. In

(15) Baker, E. N.; Hubbard, R. E. *Prog. Biophys. Mol. Biol.* **1984**, *44*, 97.

(16) Peters, D.; Peters, J. *J. Mol. Struct.* **1980**, *68*, 255.

(17) Mitchell, J. B. O.; Price, S. L. *Chem. Phys. Lett.* **1989**, *154*, 267.

(18) Prasad, D.; Sinha, V. N.; Prasad, N. *Nat. Acad. Sci. Lett. (India)* **1985**, *8*, 115.

(19) Bouchet, P.; Elguero, J.; Jacquier, R.; Pereillo, J.-M. *Bull. Soc. Chim. Fr.* **1972**, *6*, 2264.

(20) (a) Anthoni, U.; Larsen, C.; Nielsen, P. H. *Acta Chem. Scand.* **1969**, *23*, 3513. (b) Walter, W.; Reubke, K.-J. *Chem. Ber.* **1970**, *103*, 2197.

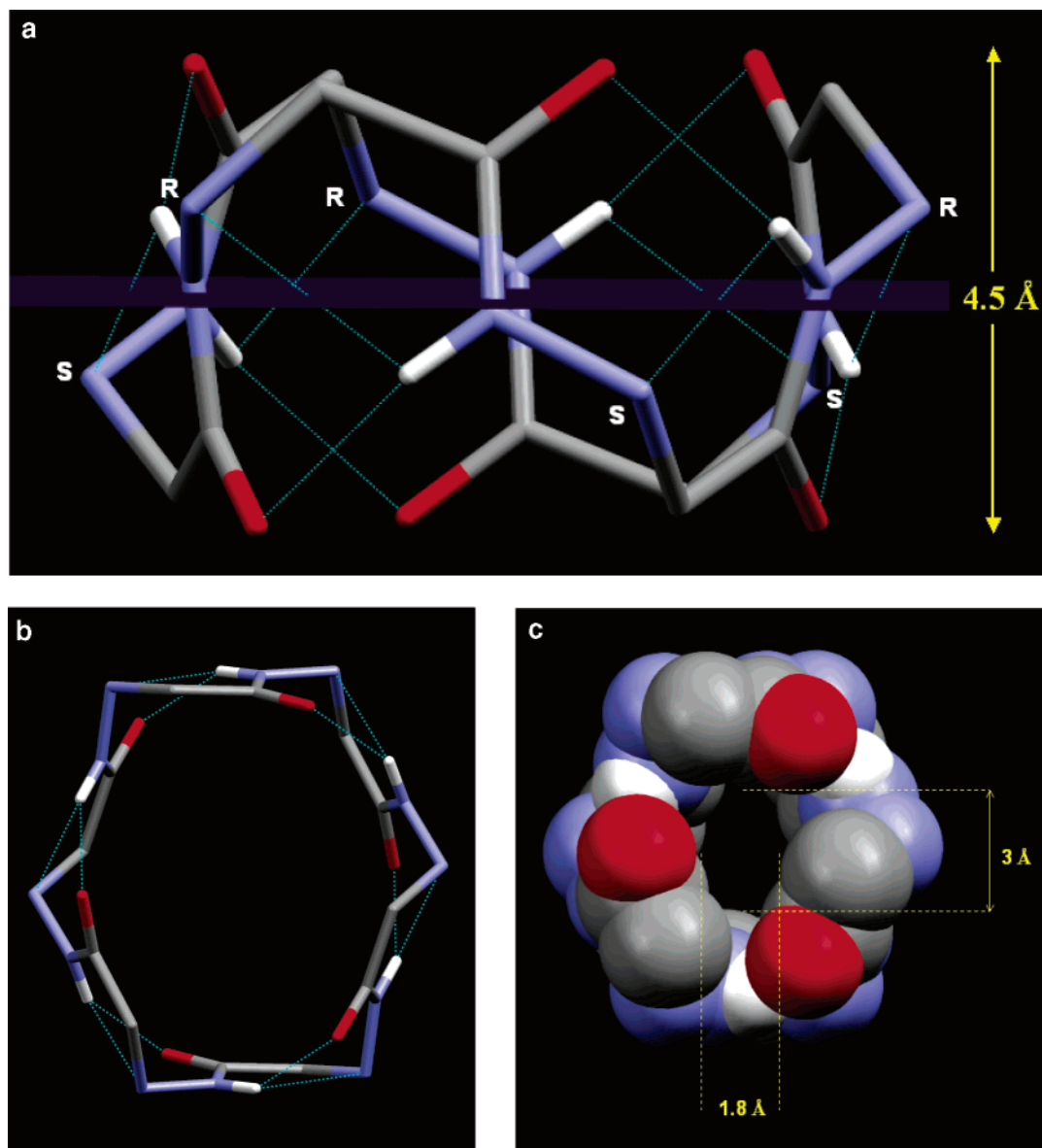


**FIGURE 8.** (a) Solid state conformation of aza- $\beta^3$ -cyclohexapeptides: side view. Side chains are omitted for clarity. (b and c) Solid state conformation of aza- $\beta^3$ -cyclohexapeptides: top view. Side chains are omitted for clarity.

**TABLE 2.** Average Torsional Angles (deg) of an *R* and an *S*-Hydrazinoturn in Aza- $\beta^3$ -Cyclohexapeptides

torsional angles	$\omega$	$\phi$	$\theta$	$\psi$
<i>R</i> -hydrazinoturn	180	+115	-90	+10
<i>S</i> -hydrazinoturn	180	-115	+90	-10

this solvent, the  $^{13}\text{C}$  data show that  $\delta\text{CO}_E$  (175.47 ppm) occurs at lower field than  $\delta\text{CO}_Z$  (169.68 ppm). The FT-IR spectrum (1 mM, DCM) shows a single CO vibration at  $1678\text{ cm}^{-1}$ , but two separate NH signals at  $3424$  and  $3303\text{ cm}^{-1}$ .

In the IR spectra of aza- $\beta^3$ -cyclohexapeptides (1 mM, DCM), the single NH stretch frequency around  $3200\text{ cm}^{-1}$  indicates

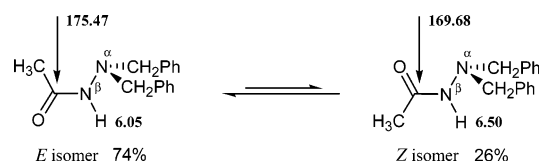


**FIGURE 9.**  $^1\text{H}$  and  $^{13}\text{C}$  NMR chemical shift (ppm) of the hydrazidic bond in the *E* and *Z* isomers of *N,N*-dibenzylacetylhydrazide **4** ( $\text{CDCl}_3$ ).

that the hydrazidic NHs remain strongly H-bonded in solution, as observed in the solid state.

The complete assignment of  $^1\text{H}$  NMR spectra is easily performed using a 2D COSY experiment. In fact, while 1D  $^1\text{H}$

**TABLE 3.** Average Distances ( $\text{\AA}$ ) and Angles (deg) of Intramolecular H-Bond in Aza- $\beta^3$ -Peptides and in Aza- $\beta^3$ -Cyclohexapeptides

intramolecular hydrogen bonds	Distances ( $\text{\AA}$ )		Angles (deg)	
	$\text{O}_i \cdots \text{HN}_{i+2}$	$\text{N}^{\alpha}_{i+1} \cdots \text{HN}_{i+2}$	$\text{O}_i \cdots \text{H}-\text{N}_{i+2}$	$\text{N}^{\alpha}_{i+1} \cdots \text{H}-\text{N}_{i+2}$
aza- $\beta^3$ -peptides	2.22	2.27	143.76	109.80
aza- $\beta^3$ -cyclohexapeptides	2.10	2.29	153.41	108.98

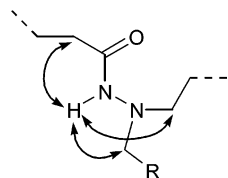


**FIGURE 10.**  $^4J$  coupling of a hydrazidic NH.

NMR spectra present sharp resonance peaks, where no long-range coupling can be detected, the bidimensional spectra show strong cross-peaks, which reveal  $^4J$  coupling between each hydrazidic NH and the nearest methylene neighbors (Figure 10).  $^{13}\text{C}$  assignment is then obtained by complementary HMQC and HMBC sequences.

The strong H-bonding of NHs shown by the IR spectroscopy results in much lower field corresponding  $^1\text{H}$  NMR signals ( $10.05 \text{ ppm} < \delta\text{NH} < 10.40 \text{ ppm}$ , 10 mM,  $\text{CDCl}_3$ ), when compared to the NH chemical shift of 6.50 ppm observed for the *Z* isomer of the model compound **4**. These hydrazidic protons are completely insensitive to dilution experiments and to the addition of increasing amounts of  $\text{DMSO-}d_6$ . The  $^{13}\text{C}$  chemical shifts of the hydrazidic carbonyl groups, around 169 ppm, indicate that the hydrazidic bonds are in the *Z* geometry. These spectroscopic observations strongly support the persistence of the network of hydrazinoturns in solution. The engagement of all H-bond donors and H-bond acceptors in intramolecular contacts also manifests in the absence of ag-

gregation phenomena with increasing concentration. Since there is no other way to maintain the hydrazinoturns' network in a cyclic aza- $\beta^3$ -hexapeptide than to adopt an alternating chiral sequence of the  $\text{N}^\alpha$  nitrogen atoms, it is clear that the general conformation of the backbone revealed by X-ray diffraction is retained in solution. This is further supported by the number of signals observed for the NMR spectra of hexamers **1**, **2**, and **3** (one, two, and three sets of signals, respectively), which reflects the  $\text{C}_3$ -symmetric conformation of the backbone. The full interconnection of the H-bond network, which leads to an optimal cooperativity effect, is also reflected in the fact that the chemical shifts of the hydrazidic protons have higher values (average value around 10.25 ppm) within the cyclic compounds than in the starting oligomers (average value around 9.50 ppm). These higher values are also probably indicative of the optimized geometry of the  $\text{CO}\cdots\text{HN}$  bond observed in the crystal structures of the macrocycles.

In contrast to the precursors, the existence of the network of hydrazinoturns in the macrocycles generates geminal anisochronism of the diastereotopic groups and the methylene protons for both the backbone and the side chains, as illustrated in Figure 11, for compound **3**. This is not so surprising considering that the rotations of the backbone, required to reverse the chiral sequence, are more difficult inside the cyclic structure.

The coalescence of signals, which then requires the interconversion between the two mirror images of the macrocycle (Figure 12), is observed only around 373 K. As the chemical

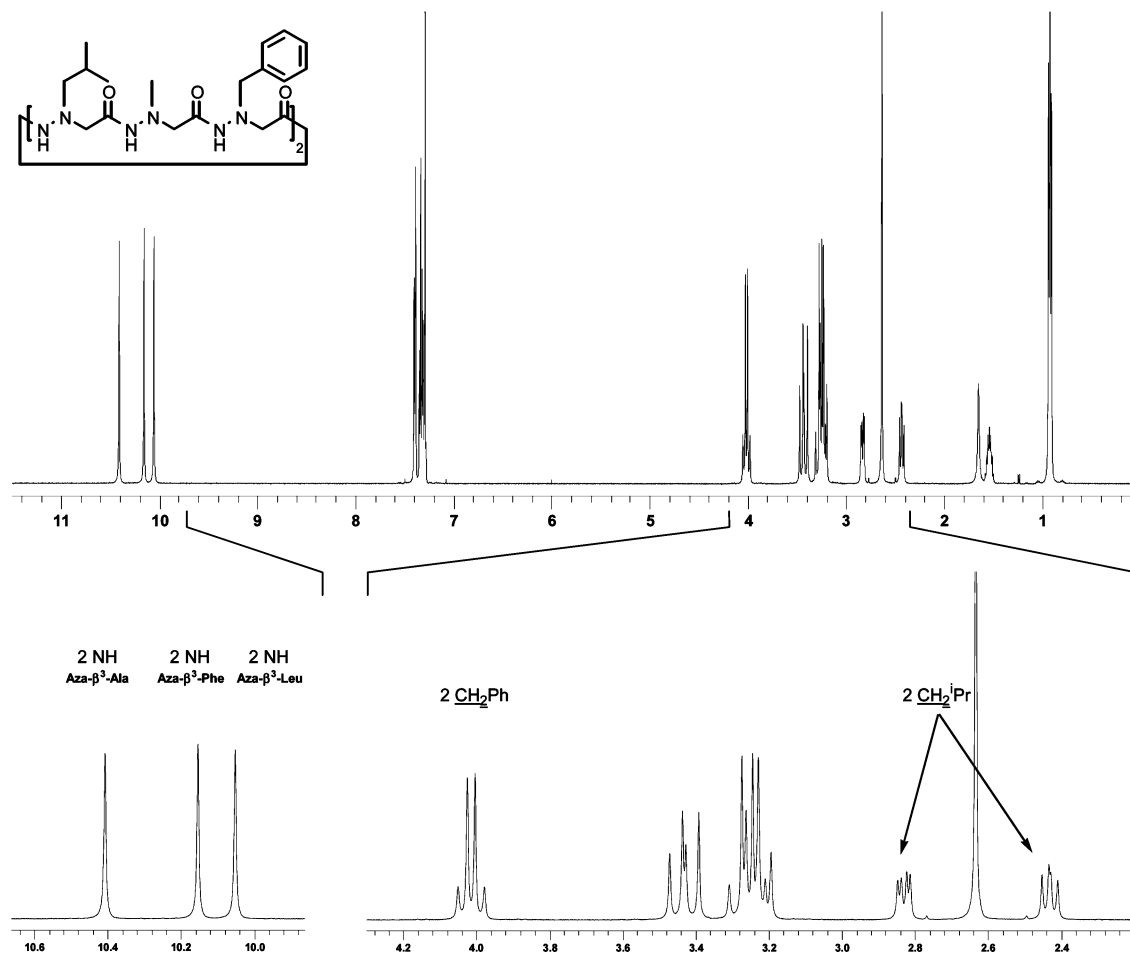


**FIGURE 11.**  $^1\text{H}$  NMR (500 MHz) spectrum of compound **3** ( $\text{CDCl}_3$ , 10 mM, 298 K).

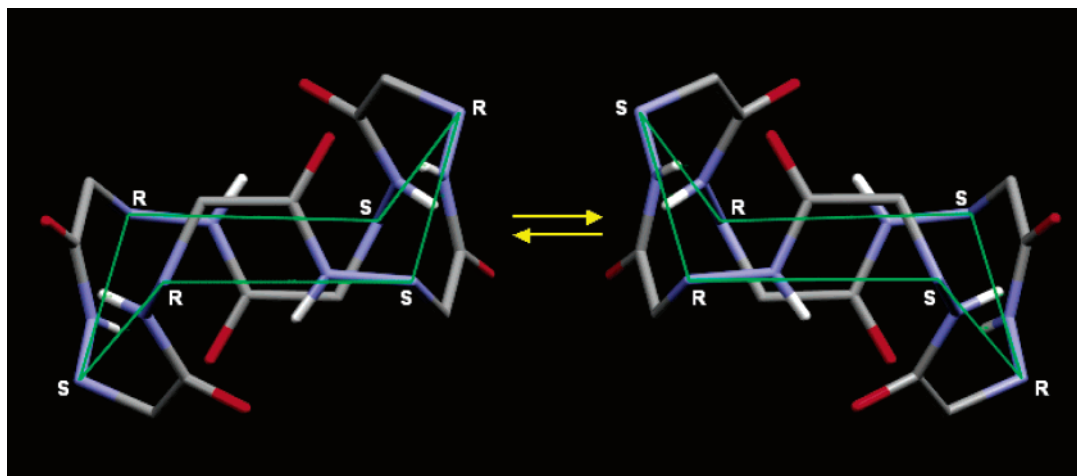


FIGURE 12. Equilibrium between the two “chair forms” of the macrocycles.

shifts of the NHs are unaffected neither by an increase nor a lowering of the temperature (from 213 to 413 K), the interchange necessarily occurs through short-lived species. This behavior is reminiscent of the interconversion between chair forms in cyclohexanes. It is especially attractive to draw this parallel because joining the N<sup>α</sup>-chiral centers strikingly reveals a perfect chair conformation (green lines in Figure 12). From a stereochemical viewpoint, the case of aza-β<sup>3</sup>-cyclohexapeptides differs from the corresponding cyclohexanes. Side chains are constrained in “equatorial” positions, and the orientation of the CONH bonds in the backbone must be taken into account. Thus, while compounds **1** and **3** are meso forms, compound **2** exists as a pair of enantiomers. Because the net result of the interchange between the two chair forms is to reverse the chiral sequence, it can be concluded that the pyramidal inversion of the N<sup>α</sup> nitrogen atoms is notably slowed in these compounds.

Slow pyramidal inversion<sup>21</sup> is commonly observed when a nitrogen atom is in a three-membered ring, where inversion has to overcome the additional tension imposed to the cycle by the sp<sup>3</sup> to sp<sup>2</sup> transition. Pyramidal inversion is further slowed when the nitrogen atom is connected to one or several atoms bearing unshared pairs of electrons, partly because of the additional energy associated with lone-pair electron repulsion that occurs during the inversion process. The combination of these two factors has even allowed slow nitrogen inversion to be detected in a five-membered ring.<sup>22</sup> However, to the best of our knowledge, aza-β<sup>3</sup>-cyclohexapeptides reveal the unprecedented

occurrence of slow nitrogen pyramidal inversion in a 24-membered macrocycle.

The temperature of coalescence, *T<sub>c</sub>*, is 353 K for **1**, 388 K for **2**, and 368 K for **3**. These values correspond to Δ*G*<sup>\*</sup> between 72.5 and 78.5 kJ/mol, comparable to those observed for *N*-alkyl aziridines.<sup>23</sup> The modulation of the *T<sub>c</sub>* values between macrocycles suggests a steric effect. However, the effect of increasing the size of an alkyl *N*-substituent in aziridines is to lower the Δ*G*<sup>\*</sup> value, that is, the inverse of what we observe for our macrocycle. Nevertheless, aza-β<sup>3</sup>-cyclohexapeptides correspond to a more complex case, and one must consider that the stereochemical inversion of these macrocycles requires the “top side” chains and “bottom side” chains to be crossed during the process. This steric effect lets us foresee that the Δ*G*<sup>\*</sup> could be increased to a level that should allow the isolation of enantiomers in compounds with bulkier substituents.

## Conclusion

Aza-β<sup>3</sup>-hexapeptides have unique conformational characteristics that display excellent predisposition to macrocyclization. This advantage results from the fact that their arrangement as successive planes, like peptides themselves, combines with their ability to reach spontaneously the favorable alternating chiral sequence during the screening of all possible diastereomeric forms. The alternating chiral sequence is maintained inside the cyclic structure by the persistence of the framework of hydrazinoturns. It follows that the macrocycles adopt a well-defined compact secondary structure like a tight fist. It is worth noting that, starting from a mixture of 32 diastereoisomers, the macrocyclization leads to a unique compound (compounds **1** and **3**) or a racemate (compound **2**), where the relative configuration of the nitrogen atoms is fixed. As the corresponding yields are excellent, this makes aza-β<sup>3</sup>-cyclohexapeptide an attractive scaffold, in particular, since C<sub>3</sub>-symmetric cyclohexapeptides have recently been shown to be functional mimetics of trimeric CD40L, the ligand of a member of the tumor necrosis factor (TNF) superfamily implied in the immune response.<sup>24</sup>

The slow pyramidal inversion of nitrogen atoms that takes place in these macrocycles was at first sight surprising as it

(21) (a) Brois, S. J. *J. Am. Chem. Soc.* **1968**, *90*, 506. (b) Brois, S. J. *J. Am. Chem. Soc.* **1968**, *90*, 508. (c) Lehn, J.-M.; Wagner, J. *Chem. Commun.* **1969**, 1298. (d) Kostyanovsky, R. G.; Samojlova, Z. E.; Tchervin, I. I. *Tetrahedron Lett.* **1969**, *9*, 719. (e) Andose, J. D.; Lehn, J.-M.; Mislow, K.; Wagner, J. *J. Am. Chem. Soc.* **1970**, *92*, 4050. (f) Rauk, A.; Allen, L. C.; Mislow, K. *Angew. Chem., Int. Ed.* **1970**, *9*, 400. (g) Kostyanovsky, R. G.; Shustov, G. V.; Zaichenko, N. L. *Tetrahedron* **1982**, *38*, 949. (h) Rudchenko, V. F.; D'yachenko, O. A.; Zolotoi, A. B.; Atovmyan, L. O.; Chervin, I. I.; Kostyanovsky, R. G. *Tetrahedron* **1982**, *38*, 961. (i) Prati, F.; Forni, A.; Moretti, I.; Torre, G.; Rozhkov, V. V.; Makarov, K. N.; Chervin, I. I.; Kostyanovsky, R. G. *J. Fluorine Chem.* **1998**, *89*, 177. (j) Kostyanovsky, R. G.; Schurig, V.; Trapp, O.; Lyssenko, K. A.; Averkiev, B. B.; Kadorkina, G. K.; Prosyaniuk, A. V.; Kostyanovsky, V. R. *Mendeleev Commun.* **2002**, *12*, 137. (k) Usachev, S. V.; Nikiforov, G. A.; Strelenko, Y. A.; Chervin, I. I.; Lyssenko, K. A.; Kostyanovsky, R. G. *Mendeleev Commun.* **2003**, *13*, 136. (l) Trapp, O.; Schurig, V.; Kostyanovsky, R. G. *Chem.—Eur. J.* **2004**, *10*, 951.

(22) (a) Müller, K.; Eschenmoser, A. *Helv. Chim. Acta* **1969**, *52*, 1823. (b) Kostyanovsky, R. G.; Kadorkina, G. K.; Kostyanovsky, V. R.; Schurig, V.; Trapp, O. *Angew. Chem., Int. Ed.* **2000**, *39*, 2938.

(23) (a) Bottini, A. T.; Roberts, J. D. *J. Am. Chem. Soc.* **1958**, *80*, 5203. (b) Anet, F. A. L.; Osyany, J. M. *J. Am. Chem. Soc.* **1967**, *89*, 352. (c) Brois, S. J. *J. Am. Chem. Soc.* **1967**, *89*, 4242.

was observed before only in small rings (three- or five-membered). Nevertheless, we have previously demonstrated that these atoms are H-bonded to hydrazidic NHs. This interaction is prone to stabilize the pyramidal ground state and therefore to increase the inversion barrier.<sup>25</sup> In macrocycles, this phenomenon combines with two new factors in contrast to the precursors, namely, the optimum cooperative effect along the uninterrupted H-bond network and the angular constraints associated with the rotation around the  $N^\beta-N^\alpha$ , and  $N^\alpha-C_\alpha$  bonds. These results show that pyramidal inversion is no more limited to small rings and opens up new perspectives in this field.

## Experimental Section

**General Macrocyclization Procedure.** The precursors of compounds **1**, **2**, and **3** were assembled from Boc-protected  $N^\alpha$ -substituted hydrazinoacetic monomers<sup>5</sup> following our previous publications.<sup>2a</sup> The only improvement consists of using EDCI/HOBT (1.2 equiv) instead of DCC/DMAP as coupling reagents. We used an unoptimized coupling time of 12 h for each step. After this time, the DCM solution was washed successively with 1 N HCl (twice), water (twice), 1 N  $\text{NaHCO}_3$ , dried on  $\text{Na}_2\text{SO}_4$ , and evaporated.

Typically, a Boc-aza- $\beta^3$ -OH hexamer (1 mmol) was treated with a mixture of DCM/TFA (6 mL/4 mL) for 4 h. The excess of TFA was then co-evaporated under reduced pressure with toluene ( $3 \times 20$  mL) then ether ( $3 \times 20$  mL) until a white foam appeared. The crude residue was dissolved in 20 mL of DCM, and 10 mmol of triethylamine was added. This solution was poured drop by drop into a solution of EDCI (8 mmol) and HOBT (8 mmol) in 1.5 L of DCM. The reaction was stirred vigorously for 48 h (unoptimized). The volume was then reduced to around 100 mL. The addition of 20 mL of 1 N HCl under stirring gave rise to the apparition of a white solid (HOBT, HCl) which was filtered by suction. The solution was then washed successively with 20 mL of 1 N HCl, twice with 20 mL of water, twice with 20 mL of 1 N  $\text{NaHCO}_3$ , dried on  $\text{Na}_2\text{SO}_4$ , and evaporated. In all cases, the crude reaction

product was obtained as a very clean white powder. The solids were washed intimately by stirring overnight in 20 mL of EtOAc. Filtration gives **1**, **2**, and **3** in 76, 75, and 77% yields, respectively. Characterization data for **3**: mp 271–273 °C;  $^1\text{H}$  NMR (500 MHz,  $298\text{ K}$ ,  $\text{CDCl}_3$ , 10 mM)  $\delta$  0.91 (d,  $J = 6.84$  Hz, 6H,  $2 \times \text{CH}_3$ ), 0.93 (d,  $J = 6.66$  Hz, 6H,  $2 \times \text{CH}_3$ ), 1.54 (n,  $J = 7.17$  Hz, 2H,  $2 \times \text{CH}$ ), 2.42 (dd,  $J = 12.07, 9.38$  Hz, 2H,  $2 \times \text{CH}_A$ ), 2.63 (s, 6H,  $2 \times \text{CH}_3$ ), 2.82 (dd,  $J = 12.07, 5.00$  Hz, 2H,  $2 \times \text{CH}_B$ ), 3.21 (d,  $J = 17.68$  Hz, 2H,  $2 \times \text{CH}_{A1}$ ), 3.23 (d,  $J = 17.28$  Hz, 2H,  $2 \times \text{CH}_{A2}$ ), 3.25 (d,  $J = 17.49$  Hz, 2H,  $2 \times \text{CH}_{A3}$ ), 3.29 (d,  $J = 17.28$  Hz, 2H,  $2 \times \text{CH}_{B2}$ ), 3.41 (d,  $J = 17.68$  Hz, 2H,  $2 \times \text{CH}_{B1}$ ), 3.45 (d,  $J = 17.49$  Hz, 2H,  $2 \times \text{CH}_{B3}$ ), 3.99 (d,  $J = 12.69$  Hz, 2H,  $2 \times \text{CH}_{A4}$ ), 4.03 (d,  $J = 12.69$  Hz, 2H,  $2 \times \text{CH}_{B4}$ ), 7.28–7.35 (m, 6H,  $4 \times \text{CH}_m, 2 \times \text{CH}_p$ ), 7.39 (d,  $J = 6.73$  Hz, 4H,  $4 \times \text{CH}_o$ ), 10.05 (s, 2H,  $2 \times \text{NH}$ ), 10.15 (s, 2H,  $2 \times \text{NH}$ ), 10.41 (s, 2H,  $2 \times \text{NH}$ );  $^{13}\text{C}$  NMR (75 MHz,  $\text{CDCl}_3$ )  $\delta$  20.76 ( $2 \times \text{CH}_3$ ), 20.93 ( $2 \times \text{CH}_3$ ), 26.87 ( $2 \times \text{CH}$ ), 47.56 ( $2 \times \text{CH}_3$ ), 59.25 ( $2 \times \text{CH}_2$ ), 62.33 ( $2 \times \text{CH}_2$ ), 62.46 ( $2 \times \text{CH}_2$ ), 63.80 ( $2 \times \text{CH}_2$ ), 68.05 ( $2 \times \text{CH}_2$ ), 128.37 ( $2 \times \text{CH}_p$ ), 128.83 ( $4 \times \text{CH}_m$ ), 129.50 ( $4 \times \text{CH}_o$ ), 136.20 ( $2 \times \text{C}$ ), 169.26 ( $2 \times \text{CO}$ ), 169.81 ( $2 \times \text{CO}$ ), 170.06 ( $2 \times \text{CO}$ ). ESI<sup>+</sup> HRMS 775.4341, calcd for  $\text{C}_{36}\text{H}_{56}\text{N}_{12}\text{O}_6\text{Na}$  775.4345.

Compound **4** was prepared following literature.<sup>19</sup> The compound was crystallized from ether: mp 88–90 °C (lit. 89 °C). Anal. Calcd: C, 75.59; H, 7.09; N, 11.02. Found: C, 75.76; H, 7.20; N, 11.17.

**Acknowledgment.** Acknowledgment is made to Thierry Roisnel from the Centre de Diffraction X of Rennes for valuable assistance in X-ray data collection, and Arthur Mar for his precious help with American language.

**Supporting Information Available:** Full characterization data for compounds **1–4**. Copies of  $^1\text{H}$  NMR and  $^{13}\text{C}$  NMR spectroscopic data. Superposition of  $^1\text{H}$  NMR spectra at different temperatures in  $\text{C}_2\text{D}_2\text{Cl}_4$  for compounds **1–3**. Graphics showing the variation of the chemical shifts of NHs as a function of the concentration of DMSO- $d_6$  in  $\text{CDCl}_3$  (0–9%) for compound **3**. Chemical shifts of NHs of compound **3** at different concentrations in  $\text{CDCl}_3$  (from 1 to 100 mM). Crystallographic details. Copies of FT-IR spectra of compounds **2** and **4** (1 mM in DCM). Superposition of  $^1\text{H}$  NMR spectra at different temperatures in  $\text{CDCl}_3$  for compound **2**. Portions of the 2D NOESY spectrum and the summary of NOEs observed for compound **4** in DMSO- $d_6$  at 298 K (s, strong NOE; w, weak NOE). Crystallographic data in CIF format for compounds **1–3**. This material is available free of charge via the Internet at <http://pubs.acs.org>.

JO0608467

(24) (a) Hymowitz, S. G.; Ashkenazi, A. *Nat. Chem. Biol.* **2005**, *1*, 353. (b) Fournel, S.; Wieckowski, S.; Sun, W.; Trouche, N.; Dumortier, H.; Bianco, A.; Chaloin, O.; Habib, M.; Peter, J.-C.; Schneider, P.; Vray, B.; Toes, R. E.; Offringa, R.; Melief, C. J. M.; Hoebeke, J.; Guichard, G. *Nat. Chem. Biol.* **2005**, *1*, 377.

(25) Stackhouse, J.; Baechler, R. D.; Mislow, K. *Tetrahedron Lett.* **1971**, *37*, 3437.